DEPENDENCE OF THE YIELD STRESSES OF CERTAIN MATERIALS ON LOADING RATE

Yu. A. Belyaev, A. F. Mel'shanov, and Yu. V. Suvorova

Zhurnal Prikladnoi Mekhaniki i Tekhnicheskoi Fiziki, Vol. 10, No. 2, pp. 136–141, 1969

The dependence of the dynamic yield stresses of certain metals and alloys on loading rate has been investigated at temperatures of +20 and −196° C. In the experiments the loading rate remained constant up to the appearance of plastic strains, i.e., $\sigma(t) = \dot{\sigma} t$, where $\dot{\sigma} = \text{const}$. The yield stresses of the materials and the time to the appearance of plastic strains were determined from the oscillograms representing the strain and load as functions of time.

1. Techniques and equipment developed in the laboratory have made it possible to conduct dynamic tensile tests at loading rates of approximately $2 \cdot 10^3$, $1 \cdot 10^6$ and $4 \cdot 10^7$ kg/mm^2 · sec (the corresponding strain rates were $1 \cdot 10^{-1}$, $5 \cdot 10$, $2 \cdot 10^3$ sec^{-1}) [1, 2]. Strain rates of the order of 10^{-1} sec^{-1} were created with a specially designed pneumatic testing machine and strain rates of the order of $5 \cdot 10$ sec^{-1} with a vertical impact tester in which a falling weight struck the lower end of the vertically mounted test piece. The test pieces used in both these cases were the same and had a guage length of 12 mm, so that the wave transit time $t = 2.4 \cdot 10^{-6}$ sec. On these machines plastic strains developed after approximately 10^{-2}–10^{-4} sec. During this interval the waves traversed the gauge length of the test piece many times and hence the wave distortions caused by reflection from the boundaries of the gauge portion had time to smooth out.

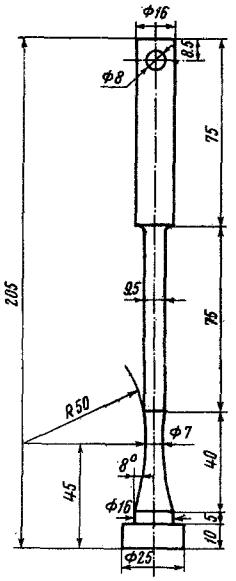

Fig. 1

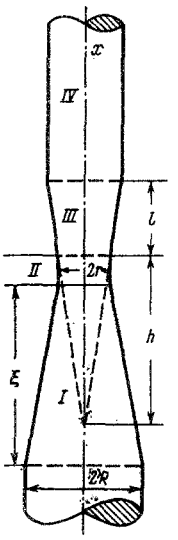

Fig. 2

A different situation exists when test pieces are deformed at higher rates (on the order of $2 \cdot 10^3$ sec^{-1}) on the pneumatic testing machine described in detail in [2]. In this case loading is effected by a weight striking at a velocity of 100 m/sec a sphere located at the end of a hollow waveguide, within which the test piece is secured. The load is transmitted through the waveguide to the lower end of the test piece, whose upper end is not gripped, but merely suspended from a pin, since the test piece is destroyed before the loading wave can travel its entire length.

The dimensions and shape of the test piece are presented in Fig. 1, and the schematization used in the following calculations is presented in Fig. 2.

It was calculated that the stress concentration coefficient resulting from the nonuniformity of the test piece cross section is only 1.05; consequently, it may be assumed that the stress distribution over the cross section is uniform.

The gauge length II is assumed equal to 4 mm – the width of the strain gauge, which was attached at the narrowest section between the two conical parts. The stress sensor was located in region IV of the test piece, where the deformation was exclusively elastic. This test piece shape and sensor arrangement was determined by the need to fix the point at which plastic deformation should first occur.

In selecting the shape of the gauge portion of the test piece the following considerations were taken into account. If the loading rate is large, the front of the wave traveling through that region is steep. Accordingly, plastic deformation may occur not in the section where the area is minimum, but nearer to the head. A rough estimate shows that for a test piece of the shape employed the loading rate should not exceed $7 \cdot 10^7$ kg/mm^2 · sec. The maximum loading rate reached in the experiments was $4 \cdot 10^7$ kg/mm^2 · sec. Thus, the necessary condition was well satisfied, and an exact analysis is not necessary.

2. In organizing the experiments it was necessary to consider not only the shape and dimensions of the test piece and the loading conditions, but also the quality and reliability of the measurements. It has already been mentioned that the stress sensor was attached in region IV of the test piece. In this connection, it was necessary to determine how the loading wave is distorted on reflection at the junction of the conical III and cylindrical IV parts of the rod and how this distortion affects the measured stress.

For simplicity, we will consider only parts III and IV of the rod, assuming that the cylindrical part IV is semi-infinite and that only direct waves are propagated in that part. We locate the coordinate origin in the center of the smaller base of conical part III. At time t = 0 let a load be applied to that base such that $\varepsilon = \dot{\varepsilon}_0 t$, where $\dot{\varepsilon}_0 = \text{const}$. This corresponds to what in fact occurs and is confirmed by the oscillograms obtained from the strain gauge and indicating the variation of strain with time in the section x = 0. It is necessary to determine how the loading wave is distorted on reflection from the bases of the cone $x = l$ and x = 0 and in what form it reaches the cylindrical part of the rod. Only direct waves are propagated in the cylindrical region IV; accordingly, we can confine our attention to the section $x = l$, since in all other sections the picture will be the same, except for a time shift, and determine in that section the time dependence of the strain $\varepsilon(t)$ and the strain rate $\dot{\varepsilon}(t)$.

For the conical III and cylindrical IV parts of the rod we can write the following wave equations and boundary and initial conditions:

for region III

$$\frac{\partial^2 u}{\partial x^2} + \frac{2}{h+x}\frac{\partial u}{\partial x} = \frac{1}{a^2}\frac{\partial^2 u}{\partial t^2} \tag{2.1}$$

$$u|_{t=0} = 0, \quad \varepsilon|_{t=0} = 0 \tag{2.2}$$

$$\varepsilon|_{x=0} = \dot{\varepsilon}_0 t \qquad \varepsilon|_{x=l} = \varepsilon(t); \tag{2.3}$$

for region IV

$$\frac{\partial^2 u}{\partial x^2} = \frac{1}{a^2}\frac{\partial^2 u}{\partial t^2} \tag{2.4}$$

$$u|_{t=l/a} = 0, \qquad \varepsilon|_{t=l/a} = 0, \qquad \varepsilon|_{x=l} = \varepsilon(t). \tag{2.5}$$

Here, $\varepsilon(t)$ is an unknown function, which must be determined. We seek the solution of Eq. (2.1) in the form [3]

$$u_{III} = \frac{\varphi(at-x) + \psi(at+x)}{h+x} \tag{2.6}$$

and that of Eq. (2.4) in the form

$$u_{IV} = f(at-x) \tag{2.7}$$

where the functions φ, ψ and f are determined from the corresponding boundary conditions.

In the section $x = l$ we have $u_{III}|_{x=l} = u_{IV}|_{x=l}$. From this we determine the function $\varepsilon(t)$; it is constructed successively for various time intervals. The first such interval begins at the instant at which the wave reaches the section $x = l$ and lasts until the instant at which the wave, returning to the section x = 0 and being reflected from it, arrives

back. This is the interval $l/a < t < 3l/a$. The duration of this and each succeeding time interval is equal to $2l/a$, which corresponds to the time in which the elastic wave is twice able to traverse the entire length of the conical part.

We start by considering the time interval $0 < t < l/a$, when the wave has not yet reached the boundary $x = l$ and there is no reflected wave: $\psi(at + x) = 0$. Using condition (2.2), we obtain the equation

$$\varphi'(z) + h^{-1}\varphi(z) + h\alpha z = 0 \quad (z = at,\ \alpha = \dot{\varepsilon}_0 / a).$$

Hence we have

$$\varphi(z) = h^2\alpha\{h[1 - \exp(-z/h)] - z\}. \tag{2.8}$$

To determine the function ψ we use condition (2.3) for the interval $l/a < t < 3l/a$ and obtain the equation

$$\psi'(z) - \frac{1}{h+l}\psi(z) + \frac{l}{h(h+l)}\varphi(z-2l) + h\alpha(z-2l) - \varepsilon\left(\frac{z-l}{a}\right)(h+l) = 0. \tag{2.9}$$

Here, $z = at + l$ and $\varphi(z-2l)$ is a function determined by expression (2.8) with z replaced by $z - 2l$. The solution of Eq. (2.9) is written

$$\psi(z) = \exp\left(\frac{z-2l}{h+l}\right)\left\{-\frac{h^2l}{2h+l}\exp\left[-\frac{(z-2l)(2h+l)}{h(h+l)}\right] + h^2\alpha(2l+h)\exp\left(-\frac{z-2l}{h+l}\right) - \right.$$
$$\left. - \frac{2h^2\alpha(h+l)^2}{2h+l} + h^2\alpha\exp\left(-\frac{z-2l}{h+l}\right)(z-2l) + (h+l)\int_{2l}^{z}\varepsilon\left(\frac{z-l}{a}\right)\exp\left(-\frac{z-2l}{h+l}\right)dz\right\}.$$

We determine the function f by means of condition (2.5):

$$f(z) = -\int_{2l}^{z}\varepsilon\left(\frac{z-l}{a}\right)dz \qquad (z = at + l).$$

Equating the displacements u_{III} and u_{IV}, given by expressions (2.6) and (2.7) at the boundary $x = l$, we obtain an integral equation for the unknown function $\varepsilon(t)$ in the expressions for ψ and f:

$$-\frac{2h^3\alpha(h+l)}{2(h+l)}\exp\left[-\frac{(z-2l)(2h+l)}{h(h+l)}\right] + 2h^2\alpha(h+l)\exp\left(-\frac{z-2l}{h+l}\right) -$$
$$-\frac{2h^2\alpha(h+l)^2}{2h+l} + (h+l)\int_{2l}^{z}\varepsilon\left(\frac{z-l}{a}\right)\exp\left(-\frac{z-2l}{h+l}\right)dz +$$
$$+(h+l)\exp\left(-\frac{z-2l}{h+l}\right)\int_{2l}^{z}\varepsilon\left(\frac{z-l}{a}\right)dz = 0.$$

The solution of this equation has the form:

$$\varepsilon(z) = \frac{2h^2\alpha}{3h+2l}\left\{\exp\left[\frac{z-2l}{2(h+l)}\right] - \exp\left(-\frac{z-2l}{h}\right)\right\}$$
$$(z = at + l,\quad 2l < z < 4l).$$

Then for the strain rate (substituting for z the corresponding expression in terms of t) we obtain

$$\dot{\varepsilon}(t) = \frac{2h^2\dot{\varepsilon}_0}{3h+2l}\left\{\frac{1}{2(h+l)}\exp\left[\frac{at-l}{2(h+l)}\right] + \frac{1}{h}\exp\left(-\frac{at-l}{h}\right)\right\}.$$

Thus, we have constructed the functions $\varepsilon(t)$ and $\dot{\varepsilon}(t)$ on the first of the time intervals investigated $l/a < t < 3l/a$. On the next interval $3l/a < t < 5l/a$, proceeding in the same way, we easily obtain

$$\dot{\varepsilon}(t) = \dot{\varepsilon}_0\left\{\left[\frac{h^3}{(3h+2l)(h+l)}\exp\left(\frac{l}{h+l}\right) - \frac{2h^2(2l-h)}{(3h+2l)^3}\right]\exp\left[\frac{at-3l}{2(h+l)}\right] + \right.$$
$$+\left[\frac{2h^2(2l-h)}{(3h+2l)^3} + \frac{2h}{3h+2l}\exp\left(-\frac{2l}{h}\right)\right]\exp\left(-\frac{at-3l}{h}\right) -$$
$$\left. - \frac{h^2(2l+h)}{2(3h+2l)^2(h+l)^2}\exp\left[\frac{at-3l}{2(h+l)}\right](at-3l) + \frac{4h}{(3h+2l)^2}\exp\left(-\frac{at-3l}{h}\right)(at-3l)\right\}.$$

In Fig. 3, by way of illustration, we have presented the time dependence of $\dot{\varepsilon}(t)/\dot{\varepsilon}_0$ ($h = 30$ mm and $l = 10$ mm, time measured in seconds). Clearly, the function falls chiefly during the first time interval, lasting 4 μsec, i.e., a single reflection of the wave from the boundary $x = l$, while the second reflection has essentially no effect on the behavior of the strain rate. The function $\dot{\varepsilon}(t)/\dot{\varepsilon}_0$ tends to a value corresponding to the ratio of the cross-sectional areas of the conical part of the rod at $x = 0$ and the cylindrical part. (For our test piece this area ratio is 0.54.) Since the

dynamic yield point in the section $x = l$ is measured 5 μsec after the wave arrives at that section, it may be assumed that the distortions caused by reflection at the junction of the conical and cylindrical parts do not affect the results.

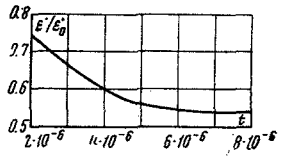

Fig. 3

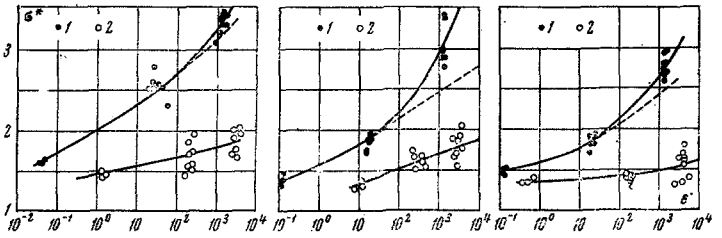

Fig. 4

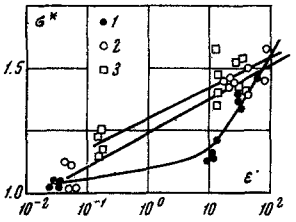

Fig. 5

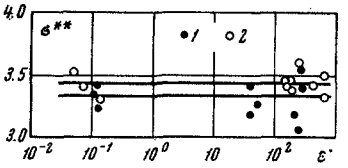

Fig. 6

3. Two groups of materials were investigated. Group A included materials whose stress-strain diagrams in uniaxial tension are characterized by a tooth and a yield plateau: armco iron, st. 3 steel, and st. 45 steel. Group B included materials whose $\sigma \sim \varepsilon$ diagram can be described by a continuously increasing function with $d^2\sigma/d\varepsilon^2 < 0$: AMG-6, OT-4, and ICr18Ni9Ti. The materials in both groups were tested at strain rates of $1 \cdot 10^{-1}$, $5 \cdot 10$, and $2 \cdot 10^3$ sec^{-1} at normal (+20° C) temperature, armco iron and st. 3 steel being also tested at −196° C. The results obtained are presented in Figs. 4, 5, and 6 (in Fig. 4 the results are given for a) armco iron, b) st. 3 steel, and c) st. 45 steel, points 1 correspond to the results obtained for the upper yield point, and points 2 to those obtained for the lower; in Fig. 5: 1−AMG-6, 2−OT-4, 3−1Cr18Ni9Ti; in Fig. 6: 1−armco iron, 2−st. 3 steel). In Figs. 4 and 5 along the axis of abscissas we have plotted the strain rate in sec^{-1}, along the ordinate axis the dimensionless quantity σ^*−the ratio of the dynamic σ_S to the static σ_0 yield stress. These graphs were obtained by analyzing the oscillograms recorded during the experiment $\varepsilon(t)$, $P(t)$ and $P(\varepsilon)$. For the materials of group A the instant at which the yield stress is reached is clearly marked and can be determined with great accuracy. As an example, Fig. 7 shows the oscillogram of a test conducted at an impact velocity of 100 m/sec (strain rate $2 \cdot 10^3$ sec^{-1}) for st. 3 steel. The points P_+ and P_- correspond to the upper and lower yield points, respectively.

For the materials of group B it was possible to determine only the yield strength corresponding to the usual set of 0.2%−$P_{0,2}$.

From the oscillograms obtained for these two groups of materials it was also possible to determine whether the condition of constancy of the strain and loading rates was satisfied and to determine their value.

It follows from Figs. 4 and 5 that, as the strain rate increases, the yield stress increases for all the materials; however, for the materials of group A the increase is more intense.

This is because the low-carbon steels in group A are characterized by delayed yield, manifested in dynamic loading and usually attributed to the motion of dislocations in an "atmosphere" of dissolved atoms. According to Campbell's criterion [4] for testing at a constant rate, the dependence of the delay time t_0 (i.e., the time from the beginning of loading to the appearance of plastic strains) on the yield stress is written as follows:

$$t_0 = C(\alpha + 1)(\sigma_s / \sigma_0)^{-\alpha}. \qquad (3.1)$$

Here, C and α are quantities depending on the temperature and composition of the material, α being a dimensionless quantity, while [C] = [t]. Since $t_0 = \sigma_S/\dot{\sigma}_0$ this formula also describes the relation between the loading (or strain) rate and the dynamic yield stress.

The experimental data on the dependence of the delay time on the magnitude and form of the loading function, the composition and properties of the materials, and temperature are reviewed in [5]. For convenience of comparison with the results of other authors presented in [5], instead of C we consider the quantity $c = C\,\sigma_0^{\alpha}$, which has the units $[kg/mm^2]^{\alpha}$. In [5] it was shown that at room temperature the value of log c may vary with the material investigated between 12 and 24, and the value of the dimensionless quantity α between 9 and 16.

From the $\varepsilon \sim \sigma_s$ graphs (Fig. 4) it is possible to calculate log c and α for the materials investigated. On the intervals of the curves from $1 \cdot 10^{-1}$ to $5 \cdot 10$ sec^{-1} (the corresponding region of delay times is $1 \cdot 10^{-2}-1 \cdot 10^{-5}$ sec) we obtain the following values: log c = 20.56, 23.80, 18.76 and α = 14.1, 16.0, 12.5, for armco iron, st. 3 steel, and st. 45 steel, respectively. These values lie within the above-mentioned intervals.

The dashed lines in Fig. 4 represent curves calculated from Eq. (3.1). Clearly, starting approximately from a value $\dot{\varepsilon} = 5 \cdot 10$ sec^{-1} (t_0 of the order of $3 \cdot 10^{-5}$ sec), the experimental points lie much higher than the calculated curves. Among the numerous studies of delayed yielding, only in Krafft's experiments [6] were such small delay times (down to 10^{-6} sec) investigated. At times less than approximately $5 \cdot 10^{-5}$ sec Krafft obtained a sharp increase in the slope of the curve characterizing the $\sigma_s \sim t_0$ dependence, which is consistent with our results.

The dependence of the lower yield point on strain rate is also shown in Fig. 4. Generally speaking, this is a conventional point, since in view of the sharp oscillations that coincide with the appearance of plastic strains (Fig. 7) it is difficult to establish from the oscillograms. However, there is no doubt that the dependence of the lower yield point σ_-/σ_0 on strain rate is much weaker than that of the upper yield point σ_+/σ_0. A similar effect was noted in [7, 8].

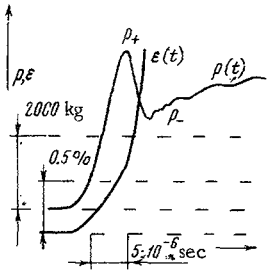

Fig. 7

In Fig. 6 the yield stress of armco iron and st. 3 steel is plotted as a function of strain rate at −196° C.

Along the axis of abscissas we have plotted the strain rate $\dot{\varepsilon}$ in sec^{-1}, and along the ordinate axis σ^{**} – the upper dynamic yield stress at −196° C divided by the upper static yield stress at +20° C. It is clear from the figure that in the range of strain rates investigated σ^{**} is a constant quantity. These results are confirmed by the work of Krafft [6, 9] and Clark and Wood [10] for the case of loading with a suddenly applied constant stress. These authors note that there is an upper stress limit, above which brittle fracture occurs and a delay effect is not observed. In the given case this limitation relates to the loading (strain) rates. Apparently, if rates lower than those investigated are considered, a tendency for σ^{**} to decrease will emerge at sufficiently small strain rates, at which loading may be assumed static, the quantity σ^{**} will be equal to the ratio of the upper static yield point at −196° C to the upper static yield point at +20° C.

REFERENCES

1. Yu. Ya. Voloshenko-Klimovitskii, The Dynamic Yield Point [in Russian], Nauka, Moscow, 1965.

2. Yu. Ya. Voloshenko-Klimovitskii, Yu. A. Belyaev, and A. F. Mel'shanov, "Equipment for testing materials at high loading rates," Zav. lab., vol. 33, no. 8, pp. 1016−1019, 1967.

3. G. S. Shapiro, "Longitudinal vibrations of rods," PMM, vol. 10, no. 5, pp. 597−616, 1946.

4. J. D. Campbell, "Dynamic yielding of mild steel," Acta Metallurgica, vol. 1, no. 6, pp. 706−710, 1953.

5. Yu. V. Suvorova, "Delayed yielding of steels (review of experimental results)," PMTF [Journal of Applied Mechanics and Technical Physics], no. 3, 1968.

6. J. M. Krafft, "Effect of temperature on delayed yielding of mild steel for short loading duration," Trans. Amer. Soc. Metals, vol. 48, pp. 249−261, 1956.

7. F. V. Warnock and D. B. C. Taylor, "Yield phenomena of a medium carbon steel under dynamic loading," Proc. Instn. Mech. Engrs, vol. 161, p. 165, 1949.

8. C. F. Elam, "The influence of rate of deformation on the tensile test with special reference to the yield point in iron and steel," Proc. Roy. Soc., London, vol. 165, pp. 568–592, 1938.

9. J. M. Krafft and A. M. Sullivan, "Effect of grain size and carbon content on the yield delay time of mild steel," Trans. Amer. Soc. Metals, vol. 51, pp. 643–665, 1959.

10. D. S. Wood and D. S. Clark, "The influence of temperature upon the time delay for yielding in annealed mild steels," Trans. Amer. Soc. Metals, vol. 43, pp. 571–586, 1951.

24 December 1968

Moscow